PCCP

Accepted Manuscript

This is an *Accepted Manuscript*, which has been through the Royal Society of Chemistry peer review process and has been accepted for publication.

Accepted Manuscripts are published online shortly after acceptance, before technical editing, formatting and proof reading. Using this free service, authors can make their results available to the community, in citable form, before we publish the edited article. We will replace this *Accepted Manuscript* with the edited and formatted *Advance Article* as soon as it is available.

You can find more information about *Accepted Manuscripts* in the Information for Authors.

Please note that technical editing may introduce minor changes to the text and/or graphics, which may alter content. The journal's standard Terms & Conditions and the Ethical guidelines still apply. In no event shall the Royal Society of Chemistry be held responsible for any errors or omissions in this *Accepted Manuscript* or any consequences arising from the use of any information it contains.

ROYAL SOCIETY OF CHEMISTRY

www.rsc.org/pccp

PCCP

RSCPublishing

ARTICLE

Surface-Enhanced Raman Scattering on a Hierarchical Structural Ag Nano-Crown Array under Different Detection Ways

Cite this: DOI: 10.1039/xoxxoooooox

Received ooth January 2014,
Accepted ooth January 2014

DOI: 10.1039/xoxxoooooox

www.rsc.org/

Yi Wang, Yuyang Wang, Hailong Wang, Ming Cong, Weiqing Xu, Shuping Xu*

A highly ordered Ag nano-crown array with a hierarchical pattern is designed as a three-dimensional (3D) surface-enhanced Raman scattering (SERS) substrate. It was achieved by depositing Ag on a patterned polymethyl methacrylate (PMMA) film which precisely replicates the patterns of a honeycomb-like anodic aluminum oxide (AAO) template. We made a detailed analysis on the structure of Ag nano-crowns and place emphasis on the detection mode to optimize the excitation and collection of the SERS signals. Finite-different time-domain (FDTD) simulation was performed to confirm and compare electric field enhancement in the gaps between nano-crowns under two different detection ways. All the results exposed and confirmed that the unique detection way of the Ag nano-crown substrate which is different from the traditional mode is optimal. This hierarchical structural Ag nano-crown not only has satisfactory repeatability, but also provides high sensitivity which was supported by the high electric field enhancement under the proper detection way. As a practical application, the detection of pesticide thiram was achieved with the limit of detection down to 1.0×10^{-14} M. This hierarchical structural Ag nano-crown array on a polymer film is a promising candidate as a portable SERS chip.

Introduction

Surface-enhanced Raman scattering (SERS) has become one of the most important modern spectroscopic methods due to its high sensitivity, non-destructive, and real-time fashion of detection.[1-6] It is found that this enormous enhancement of Raman signal is originated from the electromagnetic amplification on a variety of noble metallic nanostructures.[7-9] The design of novel metallic nanostructures is one of main trends in SERS studies since SERS signal is extremely sensitive to the morphology and size of the plasmonic nanostructure, especially the gaps between nanostructures.[3, 10] Benefiting from the advances in nanofabrication and nanomachining, many unique nanostructures have been extensively reported.[11-14] Within these nanostructures, the two-dimensional (2D) membrane-typed SERS substrates or solid-supported substrates gain great attention due to their practicality and universality in SERS detections.[15]

State Key Laboratory of Supramolecular Structure and Materials, Jilin University, Changchun, 130012, People's Republic of China
Tel: +86-431-85168505 E-mail: xusp@jlu.edu.cn
Electronic supplementary information (ESI) available. See DOI: 10.1039/x0xx00000x

The progress in these 2D solid-supported substrates started from many disordered and unartificial metallic nanostructures, such as the vacuum deposition Ag island film[16] and the metal nanoparticle assembled film.[17]

To consider about the reproducibility of SERS substrates, the ordered and periodic structures have been developed, for instant, a regular metal coating layer over a nanosphere array developed by Van Duyne,[18] the ordered metallic array by electron beam lithography[19] and focused ion-beam lithography.[20] Recently, the 3D SERS substrates attracted great interests.[3,21-25] These metallic nanostructures share a feature of the multi-scaled configuration in 3D space, which is supposed to produce more hot spots due to the addition of one dimension. This 'hot spot' structure can concentrate the incident electromagnetic field and effectively amplify the near field in the vicinity of the nanostructures.[26-28] Moreover, owing to the versatility and flexibility in 3D construction, 3D SERS substrates usually possess the adjustable gaps of plasmonic objects between edges or shape corners,[29, 30] allowing for an optimization of electromagnetic coupling to ensure strongest SERS. However, beside the prosperity in the construction of 3D SERS substrates, one key point is always missing that the SERS excitation and

Physical Chemistry Chemical Physics Accepted Manuscript

collection ways for a 3D substrate still follow the habit for a 2D SERS substrate, in which a 180 °backscattering detection mode is set for most SERS trials and the focused beams are laid on the substrates' surfaces. Since the SERS substrates have been extended to 3D, we should adopt more helpful detection ways by the reconsideration of their spatial geometries.

The excitation and collection of SERS spectra on a SERS substrate strictly rely on its plasmonic property. Finite-difference time-domain (FDTD) and other numerical simulation methods help us to disclose the local electric field distribution around metal surface and the far field coupling. By the guiding of simulation results, we can identify an optimal spatial angle to excite and collect SERS signal, especially for a 3D plasmonic nanostructure.[31] In addition, we can further pre-program a plasmonic structure to a designed SERS emission angle, achieving directional SERS.[32]

In this paper, we designed and fabricated a highly ordered Ag nano-crown array with a hierarchical pattern as a 3D SERS substrate. It was prepared by vacuum depositing Ag on a patterned finger-like polymethyl methacrylate (PMMA) film, which was achieved by precisely replicating the patterns of a honeycomb-like anodic aluminum oxide (AAO) template. The gaps between nano-crowns were controlled by adjusting the thickness of deposited Ag, in order to build more 'hot spots'. It is worth emphasizing that we paid more attention to the detection mode to optimize the excitation and collection of the SERS signals, which is different from the traditional composite SERS substrate. Under two different detection ways, the electric field in the gaps between nano-crowns was simulated by the FDTD method. What's interesting is that the signal collected from backside is better than the observe side. This hierarchical structural Ag nano-crown not only has satisfactory repeatability, but also provides high sensitivity which was supported by the high electric field under the proper detection way. As a practical application, the detection of a pesticide (thiram) was achieved with the limit of detection down to 1.0×10^{-14} M.

Experimental section

Fabrication of Ag nano-crown Array

A hierarchical structural Ag nano-crown array was fabricated by vacuum evaporating Ag film on a patterned PMMA film which had the structure replicated from a honeycomb-like anodic aluminum oxide (AAO) template (see Fig.1a). The anodic aluminum oxide (AAO) template for the formation of Ag nanocrown was fabricated with method that reported in our previous work.[33] Polystyrene (PS) nanospheres in 500 nm diameter was synthesized by emulsion polymerization method and served as a preset mold on an Al foil substrate (99.999% purity, 0.2 mm in thickness, 1.0 cm × 1.5 cm in area) via an interface self-assembly method. Reactive ion etching (RIE) (Plasmab lab 80 Plus) was used to reduce the diameter of PS nanospheres. An 80 nm thickness of Al film was deposited onto the PS spheres. The pre-patterned Al foil was anodized under the voltage of 100 V in 0.3 M phosphoric acid solution to obtain the hierarchical structural AAO template. Polymethyl methacrylate (PMMA) solid (996 K, from Sigma-Aldrich) was dissolved in dichloromethane for spin coating on AAO template. The PMMA film which had the structure replicated from hierarchical structural AAO template was cured under 130 ℃ for 30min. In order to separate the PMMA film from the AAO template, we used a copper chloride ($CuCl_2$) and hydrochloric acid (HCl) solution to remove Al and 0.1 M NaOH to remove AAO. Then, we achieved the highly ordered Ag nano-crown array structure over the flexible PMMA film by vacuum evaporating different amount of Ag on the patterned PMMA film. To distinguish them, we used the average thickness of Ag film (which is measured by a quartz crystal monitor in the vacuum deposition process) to represent these samples.

Characterization

The surface morphologies of the samples were investigated by a scanning electron microscope (SEM, HITACHI SU8020), the accelerating voltage is 3.0 kV. The reflection spectra of the Ag nano-crown array and PMMA film were measured by an Ocean Optics USB4000 spectrometer to evaluate the plasmonic properties. A halogen tungsten lamp with the power of 6.5 W was used for illumination and an Ag mirror was used as a reference. The parameters for recording the reflection spectra were as follows, integration time of 100 ms, scans to average of 8 and a boxcar width of 10. The absorption spectra were measured by an Ocean Optics USB-ISS-UV/VIS spectrometer, integration time of 10 ms, scans to average of 10 and a boxcar width of 10.

SERS spectra from the Ag nano-crown array substrates were acquired by an optical fiber portable Raman spectrometer (B&W Tek Inc.) at a backscattering mode. The excitation source was a 532 nm laser, and the integration time was 1 s. The laser power is 3.2 mW and diameter of the laser spot is about 1.0 μm. All spectra were obtained under the same conditions if not specially pointed out. As for the SERS detection, 5.0 μL of 4-mpy aqueous solution (1.0×10^{-5} M) was dropped on a 1.0 cm × 1.5 cm flexible Ag nano-crown substrate, and we collected SERS signal after the 4-mpy aqueous solution was dried. For the experiment of reproducibility, a 1.0 cm × 1.5 cm substrate was immersed in 1.0×10^{-7} M 4-mpy aqueous solution for 20 min, dried by nitrogen after clearing with water. Moreover, 5.0 μL of thiram methanol solution (1.0×10^{-6} M - 1.0×10^{-14} M) was dropped on the 3D SERS substrate, the integration time was 10 s.

FDTD Simulations

Three-dimensional finite-different time-domain (FDTD) simulations were carried out by FDTD solutions software (Lumerical Solutions, Inc.). It is used for displaying the electromagnetic (EM) field distributions around hierarchical structural Ag nano-crown array. The dielectric constant of Ag was according to Palik. The fractive index of the PMMA is 1.49. The simulation area was 450 nm × 780 nm × 630 nm with the Yee cells of 1 nm × 1 nm × 2 nm, which is sufficient

Physical Chemistry Chemical Physics Accepted Manuscript

 This journal is © The Royal Society of Chemistry 2014

to characterize the feature size of the given geometry. The boundary conditions were anti-symmetric in X-axis, symmetric in Y-axis and PML (perfectly matched layer) in Z-axis. Period spacing of the hexagonal structure is 20 nm. The gap between outer six Ag nano crowns is 10 nm. Diameter of central Ag nano crown is 100 nm and the spacing between central and outer Ag nanocrown is 10 nm. The incident wavelength is 532 nm with polarization direction parallel to X-axis, and the incident direction is vertical to the substrate surface.

Results and discussion

Morphology of the Ag nano-crown substrate

The fabrication procedure of the Ag nano-crown array is shown in Fig. 1a. First, a hierarchical structural AAO template was prepared by electrochemical anodic oxidation, which has been reported in our previous work.[33] Then, we spin-coated a PMMA layer over the AAO template (about 0.4 mm thick) and then it was peeled off. The PMMA film replicated the hierarchical structure, forming a hierarchical structural Ag nanrod array. Next, we evaporated Ag with a certain thickness on the patterned PMMA film.

Fig. 1d-f shows SEM images of the top view of the obtained substrates in each step. Fig. 1d is the AAO template and we can see it displays a honeycomb-like structure with seven holes in one unit and has almost no much breaking and defects. After PMMA copying, the hierarchical channel structure became an array of seven gathering nano-fingers (Fig. 1e). To deposit Ag on this PMMA nano-finger array, a hierarchical Ag nano-crown array was achieved over the PMMA (Fig. 1f). The period of the submicro lattice is 500 nm, and each submicro lattice consists of six symmetric bigger nano-crowns and a smaller central one. As we have concluded in previous publications,[33] the formation of the unique structure can be attributed to growth induction of the submicro nano-indentations pre-patterned on the Al surface after a "defect anodization"process,[14] which is the origin of the dimension scale of the Ag nano-crown array.

Next, we used this Ag nano-crown array with sophisticated spatial structure as a 3D SERS substrate because the precise pattern and narrow gaps may satisfy the high SERS requirements on sensitivity and reproducibility. In addition, we adopted two kinds of detection modes for this 3D substrate (Fig. 1b and c). We detected and compared SERS signals from either of two sides as shown in Fig. 1b and 1c (type Ⅰ; vertical detection from the air side. type Ⅱ; vertical detection from the adherent PMMA side). Owing to the excellent light transmittance of PMMA, few signal interference in Raman spectra was observed (see the Raman spectrum of PMMA in Fig. S1).

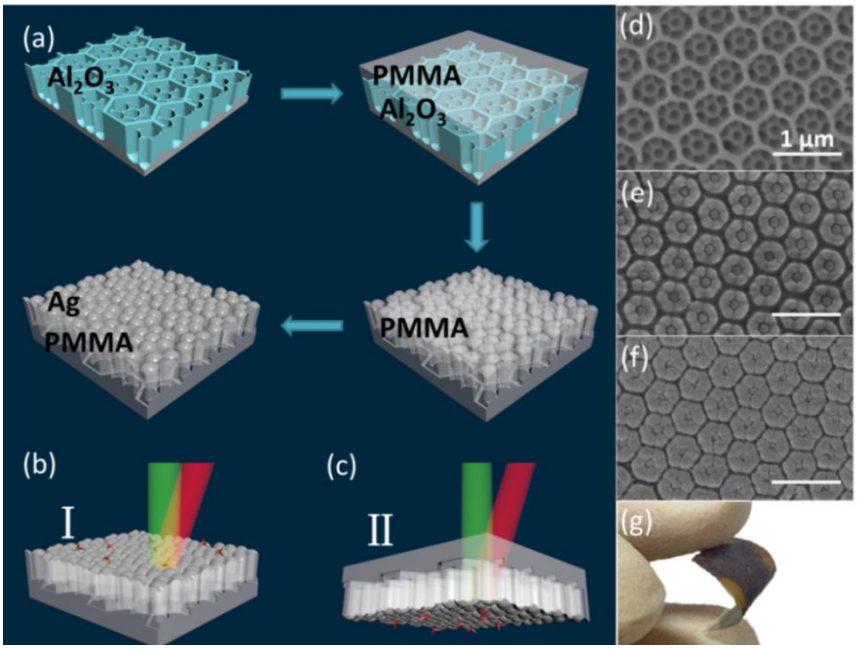

Fig. 1 (a) Preparation process of Ag nano-crown array. (b) and (c) Two types of incident modes (Type Ⅰ: detection from the air side. Type Ⅱ: detection from the PMMA side). (d) – (f) SEM images of a hierarchical structural AAO template, a PMMA film that reduplicats the AAO template and an Ag nano-crown array. The scale bar is 1 μm. (g) A photograph of an Ag nano-crown array above the PMMA film.

Different amounts of deposited Ag result in various morphologies above the finger-like PMMA film and we can regulate the gaps between nanocrowns by the amount of deposited Ag (Fig. 2). Before Ag deposition, the patterns are ordered with hexagonal structure as a unit. Because of the unique morphology of nano-finger array and the uncertainty about the nucleation sites in the process of vacuum evaporating, the deposited Ag would be nonuniform at different sites. It prefers to locate at prominence sites rather than the sunk parts. So, it forms discrete and non-uniform Ag film when the amount of deposited Ag is small (e.g. 10 and 20 nm, Fig. 2a and 2b). The structure was composed of central and outer six nano-

Physical Chemistry Chemical Physics Accepted Manuscript

crowns which retained the hierarchical pattern perfectly. The spacing between two nano crowns in Fig. 2a is 20 nm and it decreases to 10 nm in Fig. 2b, while their period spacing distances of hexagonal unit are 50 and 30 nm, respectively. When the thickness of Ag film was added up to 50 nm, the boundaries between the outer six nano-crowns became vague and almost disappeared, the periodic structure was formed by an outer hexagon and a center nano-crown (Fig. 2c). With the increase of the Ag film thickness, the structure of hierarchical period gradually disappeared, and the period spacing of hexagonal unit decreased from 30 nm to 20 nm. When the Ag film was 300 nm, the morphology tends to be a rough silver film and no obviously hierarchical structure is identifiable (Fig. 2f).

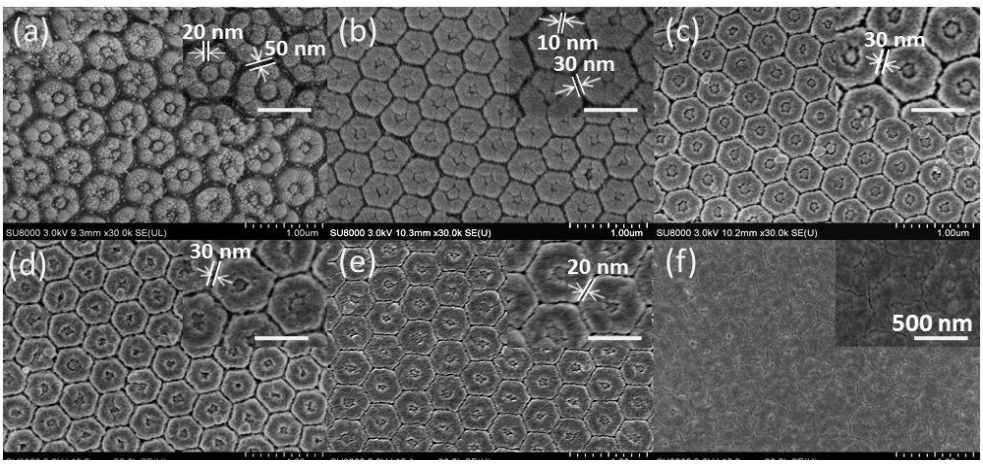

Fig. 2 SEM images of fabricated Ag nano-crown arrays with different thickness of Ag films. (a) - (f) corresponds to 10, 20, 50, 100, 200 and 300 nm, respectively. The scale bar is 500 nm.

The plasmon resonance band and excitation laser

SERS activity of a substrate is strongly affected by its plasmonic property. In order to learn about the plasmonic property of the designed 3D SERS substrate, we measured the absorption spectra of the Ag nano-crown substrate (Fig. 3a). It can be found that the absorption band is broad and located at 495 nm. The broad plasmon band allows for many choices of the laser wavelengths to couple surface plasmonic resonance for SERS excitation. In present study, we adopted a 532 nm laser for SERS excitation.

Fig. 3(b) displays the reflection spectra of two surfaces of the Ag nano-crown array substrate. It can be found that the reflectivity recorded as type Ⅱ mode has a relatively low reflectivity in the wavelength range of 350-800 nm. However, for the other surface, the Ag/air surface, the reflection is quite strong in the range of visible range. The strong reflection would decrease the light coupling efficiency in a certain degree. The relationship between the plasmon resonance and electromagnetic enhancement would be discussed later.

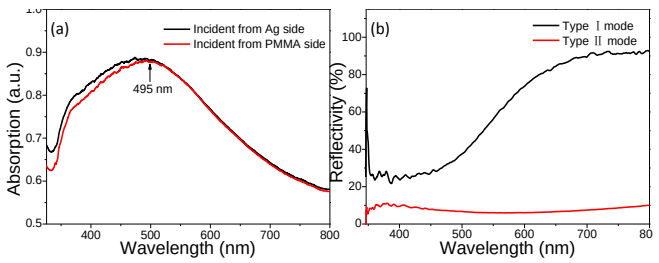

Fig. 3 (a)The absorption of a Ag nano-crown array. (b) Reflection spectra of Ag nano-crown array detected by type Ⅰ mode and type Ⅱ mode.

Control of the gaps between nano-crowns

The enhanced effect of SERS signal is crucially dependent on the size of the gaps between nano-crowns which were controlled by adjusting the thickness of Ag film. In order to find In order to find the optimal gap between nano-crowns and the optimal thickness of Ag film that can achieve the greatest enhancement, SERS spectra were collected by dropping 5.0 μL of a 4-mpy aqueous solution (1.0×10^{-5} M) on the Ag nano-crown array. The averaged SERS spectra of 4-mpy which were collected on the six substrates with different thicknesses of Ag films are shown in Fig. 4a and 4b, corresponding to the detection ways of types Ⅰ and Ⅱ, respectively. The main peaks of 4-mpy at 1001, 1053, 1086, 1216, 1569 cm^{-1} can be assigned to the ring breathing, C-N-C and C-C-C symmetry vibration, ring breathing/C-S stretching mode, C-H in plane bending, C=C stretching mode, respectively.[34] The SERS signals were enhanced evidently when the thickness of Ag film was added from 10 nm to 20 nm, corresponding to the gap of Ag nano-crown decreases from 20 to 10 nm. And then the SERS signals decrease when the thickness of Ag film is in the range of 20-60 nm with the gaps between the outer six nano-crowns disappearing. Fig. 4c shows the plots of SERS intensity at 1001 cm^{-1}. The substrate with 10 nm nanogap (20 nm thickness) is proved to have a maximal enhancement which is far higher than others, indicating a better SERS activity. We attribute the strong SERS activity to the formation of proper sized nanogaps.

Moreover, a flat Ag film with a thickness of 20 nm was prepared for SERS effect comparison between planar Ag film and the nanostructured Ag film (shown in Fig. S2). The

Physical Chemistry Chemical Physics Accepted Manuscript

This journal is © The Royal Society of Chemistry 2014

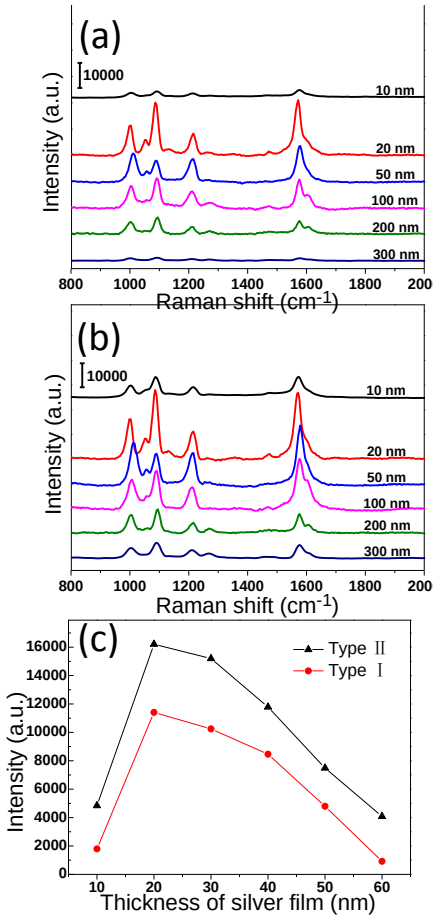

Fig. 4 (a) and (b) SERS spectra of 4-mpy which were collected on the six substrates with different thicknesses of Ag films under the detection ways of type Ⅰ and type Ⅱ, respectively. (c) SERS intensities at 1001 cm^{-1} under the two detection ways.

enhancement of the 3D substrate is about 800 times greater than the flat Ag film, indicating an excellent enhancement of SERS signal by the unique structure. The nano-crown substrate with a 20 nm Ag film was selected for subsequent experiments to testify the optimal SERS detection mode and reproducibility.

Discussion about the detection mode

As stated above, two kinds of laser irradiation ways cause difference on SERS enhancement. We compared the SERS performances of six substrates with different amount of deposited Ag under the two different detection ways (Fig. 4c and S3) and they all show the SERS signal comparison as type Ⅱ > type Ⅰ. In order to optimize the detection modes and understand where the difference of SERS performance brought from, we used the FDTD method to simulate the distributions of electric field of this substrate with laser irradiation from two sides.

Fig. 5a shows the model of the structure. We used the trial of 20 nm thickness Ag film as a sample, which supports the strongest SERS. Since the nanogaps (either between the outer six nano-crowns or between two nanofingers) decrease with the amount of deposited Ag increased, we add a thin Ag layer[35] to the side of nanofingers to present the spread Ag (see Fig. S5). The nanostructure features in XY-plane can change with the movement of Z-axis. We selected four positions in Z-axis to observe the changes of electric field: (1) the top surface of Ag nanostructure, (2) the middle plane of the Ag film, (3) the interface of PMMA/Ag film, and (4) the bottom plane of Ag which is located in the gaps (the XY-views of the four positions are shown in Fig. 5b). Fig. 5c and 5d correspond to the simulation results of the four planes with different incident directions of laser, respectively. The simulation results show that the electric field enhancement of type Ⅰ (Fig. 5c) occurs at the gaps between nano-crowns, the highest electric field intensity arrives in 1.0×10^2, and SERS enhancement factor is estimated to be on the magnitude of 10^6-10^8. The similar distributions of electric field enhancement are observed in type Ⅱ (Fig. 5d), except that the electric field intensities are much higher than type Ⅰ. The electric field intensity is as large as 1.0×10^3 of the incident light field. SERS enhancement factor is estimated to be 10^8-10^{12}. This phenomenon is in conformity with experimental SERS results exposes that the detection mode of type Ⅱ is optimal for this Ag nano-crown array.

Aimed at the differences of two detection modes, we made analysis about the plasmonic properties of this hierarchical Ag nano-crown array. Based on the above mentioned reflection

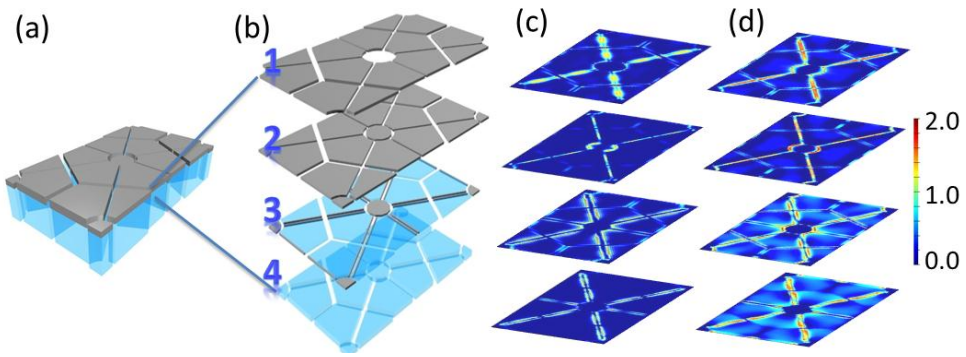

Fig. 5 3D simulation of a unit cell of the silver nano-crown. (a) The model of the nanostructure. (b) XY-view of the selected four positions in Z-axis. The simulation results of the four nanostructures with different incident direction of laser (c) type Ⅰ and (d) type Ⅱ.

Physical Chemistry Chemical Physics Accepted Manuscript

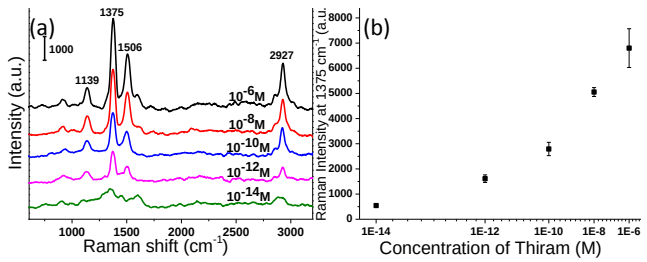

Fig. 6 (a) Concentration-dependent SERS spectra of thiram. (b) The plot of SERS intensity vs thiram concentration. The errors are from the difference of multiple spectrum.

spectra (Fig. 3b), the type Ⅱ mode has stronger light harvesting effect due to a relatively low reflectivity in visible range. The spread Ag in the gaps of nanocrowns arranged periodically and increased the roughness at the interface of Ag and PMMA, which reduced the light reflection.[36-38] However, in type I mode, the strong reflection cause a low light coupling efficiency. Accordingly, weaker SERS intensity was observed in type Ⅰ mode. Therefore, we attribute the difference between two detection modes to the different efficiencies of light harvesting at two surfaces.

Practical application of the substrate

To further demonstrate practical application of the flexible substrate, we performed the SERS detections of thiram, a toxic chemical widely used as pesticide which is irritative to skin and mucosa.[39] The SERS spectra of thiram collected on the SERS substrate are shown in Fig. 6a and a plot of SERS intensity with the thiram concentration is presented in Fig. 6b. The detected concentration range is from 1.0 μM to 10 fM. The LOD is 1.0×10^{-14} M close to femtomole scale and the signal to noise ratio is 3.0. Compared with the previously reported Ag nanoshells system which has a uniform layer of Ag shells on silica core particles, the LOD of thiram detected by Ag nano-crown array (1.0×10^{-14} M) is far better than that of the Ag nanoshells (1.0×10^{-8} M).[40] Moreover, this flexible substrate is highly ordered since it replicated the morphology of the AAO template. This should enable an even distribution of SERS "hot-spots", bringing good repeatability. We also investigated its reproducibility in SERS detections (Fig. S4) and the relative standard deviations (RSDs) of SERS intensities are less than 16%, which can meet the standard of a high-performance SERS substrate (RSDs < 20 %).[1, 12]

Conclusions

In summary, we designed a highly ordered silver nano-crown array with a hierarchical pattern as 3D SERS substrate and placed emphasis on the detection mode to optimize the excitation and collection of the SERS signals. FDTD simulation was performed to confirm and compare electric field enhancement in the gaps between nano-crowns under two different detection ways. All the results exposed and confirmed that the unique detection way which excite and collect SERS spectra from the solid-supported side is optimal due to a large light harvesting effect. This hierarchical structural Ag nano-crown not only has satisfactory repeatability, but also provides high sensitivity which was supported by the high electric field enhancement under the proper detection way. This Ag nano-crown SERS substrate with sophisticated structure can also be used in practical. Detection of thiram was achieved with a LOD down to 1.0×10^{-14} M.

Acknowledgements

This work was supported by the National Natural Science Foundation of China Grant (Nos. 21373096), National Instrumentation Program (NIP) of the Ministry of Science and Technology of China No. 2011YQ03012408, and Innovation Program of the State Key Laboratory of Supramolecular Structure and Materials, Jilin University.

Notes and references

1. M. J. Natan, *Faraday Discuss.*, 2006, **132**, 321-328.
2. K. A. Willets and R. P. Van Duyne, *Annu. Rev. Phys. Chem.*, 2007, **58**, 267-297.
3. H. Ko and V. V. Tsukruk, *Small*, 2008, **4**, 1980-1984.
4. S. M. Nie and S. R. Emory, *Science*, 1997, **275**, 1102-1106
5. M. Fleischmann, P. Hendra and A. McQuillan, *Chem. Phys. Lett.*, 1974, **26**, 163-166.
6. D. L. Jeanmaire and R. P. Van Duyne, J. *Electroanal. Chem. Interfacial Electrochem.*, 1977, **84**, 1-20.
7. P. Etchegoin, L. F. Cohen, H. Hartigan, R. J. C. Brown, M. J. T. Milton and J. C. Gallop, *J. Chem. Phys.*, 2003, **119**, 5281-5289.
8. A. Otto, I. Mrozek, H. Grabhorn and W. Akemann, *J. Phys. Condens. Matter*, 1992, **4**, 1143.
9. C. L. Haynes, A. D. McFarland and R. P. Van Duyne, *Anal. Chem.* 2005, **77**, 338 A-346 A.
10. Z. Q. Tian, B. Ren and D. Y. Wu, *J. Phys. Chem. B*, 2002, **106**, 9463-9483.
11. G. A. Baker and D. S. Moore, *Anal. Bioanal.Chem.*, 2005, **382**, 1751-1770.
12. X.-M. Lin, Y. Cui, Y.-H. Xu, B. Ren and Z.-Q. Tian, *Anal. Bioanal.Chem.*, 2009, **394**, 1729-1745.
13. Y. Yokota, K. Ueno and H. Misawa, *Small*, 2011, **7**, 252-258.
14. M. Cong, Y. Y. Wang, X. N. Wang, Y. Wang, S. P. Xu and W. Q. Xu, RSC Advances, 2014, 4, 45147-45150.
15. W. G. Xu, X. Ling, J. Q. Xiao, M. S. Dresselhaus, J. Kong, H. X. Xu, Z. F. Liu and J. Zhang, *PNAS*, 2012, **109**, 9281-9286.
16. D. A. Weitz, S. Garoff and T. J. Gramila, *Opt. Lett.*, 1982, **7**, 168-170.
17. Y. Yang, S. Matsubara, L. Xiong, T. Hayakawa and M. Nogami, *J. Phys. Chem. C*, 2007, **111**, 9095-9104.
18. L. A. Dick, A. D. McFarland, C. L. Haynes and R. P. Van Duyne, *J. Phys. Chem. B*, 2002, **106**, 853-860.
19. N. A. Abu Hatab, J. M. Oran and M. J. Sepaniak, *Acs Nano*, 2008, **2**, 377-385.
20. A. A. Tseng, *Small*, 2005, **1**, 924-939.

Physical Chemistry Chemical Physics Accepted Manuscript

This journal is © The Royal Society of Chemistry 2014

21. A. Gopalakrishnan, M. Chirumamilla, F. De Angelis, A. Toma, R. P. Zaccaria and R. Krahne, *ACS nano*, 2014, **8**, 7986-7994.
22. S. Chang, Z. A. Combs, M. K. Gupta, R. Davis and V. V. Tsukruk, *ACS Appl. Mater. Interfaces*, 2010, **2**, 3333-3339.
23. S. Chang, H. Ko, S. Singamaneni, R. Gunawidjaja and V. V. Tsukruk, *Anal. Chem.*, 2009, **81**, 5740-5748.
24. H. Liu, Z. Yang, L. Meng, Y. Sun, J. Wang, L. Yang, J. Liu and Z. Tian, *J. Am. Chem. Soc.*, 2014, **136**, 5332-5341.
25. X. Wang, S. Xu, H. Li, J. Tao, B. Zhao and W. Xu, *J. Raman Spectrosc.*, 2012, **43**, 459-463.
26. K. L. Wustholz, A. I. Henry, J. M. McMahon, R. G. Freeman, N. Valley, M. E. Piotti, M. J. Natan, G. C. Schatz and R. P. Van Duyne, *J. Am. Chem. Soc.*, 2010, **132**, 10903-10910.
27. L. D. Qin, S. L. Zou, C. Xue, A. Atkinson, G. C. Schatz and C. A. Mirkin, *PNAS*, 2006, **103**, 13300-13303.
28. H. Y. Liang, Z. P. Li, Z. X. Wang, W. Z. Wang, F. Rosei, D. L. Ma and H. X. Xu, *Small*, 2012, **8**, 3400-3405.
29. M. Hu, F. S. Ou, W. Wu, I. Naumov, X. Li, A. M. Bratkovsky, R. S. Williams and Z. Li, *J. Am. Chem. Soc.*, 2010, **132**, 12820-12822.
30. F. S. Ou, M. Hu, I. Naumov, A. Kim, W. Wu, A. M. Bratkovsky, X. Li, R. S. Williams and Z. Li, *Nano Lett.*, 2011, **11**, 2538-2542.
31. H. Guo, D. Jiang, H. Li, S. Xu and W. Xu, *J. Phys. Chem. C*, 2013, **117**, 564-570.
32. H. Li, Y. Gu, H. Guo, X. Wang, Y. Liu, W. Xu and S. Xu, *J. Phys. Chem. C*, 2012, **116**, 23608-23615.
33. X. Wang, S. Xu, M. Cong, H. Li, Y. Gu and W. Xu, *Small*, 2012, **8**, 972-976.
34. J. W. Hu, B. Zhao, W. Q. Xu, B. F. Li and Y. G. Fan, *Spectrochim. Acta, Part A*, 2002, **58**, 2827-2834.
35. W.-D. Li, F. Ding, J. Hu and S. Y. Chou, *Opt. Express*, 2011, **19**, 3925-3936.
36. I. Pockrand, *Surf. Science*, 1978, **72**, 55.
37. C. F. Eagan, W. H. Weber, *Phys Rev.*, 1979, **B19**, 5068.
38. D. Hornauer, H. Raether, *Opt. Comm*., 1973, **7**, 297.
39. X. Zheng, Y. Chen, Y. Chen, N. Bi, H. Qi, M. Qin, D. Song, H. Zhang and Y. Tian, *J. Raman Spectrosc.*, 2012, **43**, 1374-1380.
40. J.-K. Yang, H. Kang, H. Lee, A. Jo, S. Jeong, S.-J. Jeon, H.-I. Kim, H.-Y. Lee, D. H. Jeong, J.-H. Kim, and Y.-S. Lee, *ACS Appl. Mater. Interfaces*, 2014, **6**, 12541−12549.

Physical Chemistry Chemical Physics Accepted Manuscript